Topological Entanglement-Spectrum Crossing in Quench Dynamics

Zongping Gong[1] and Masahito Ueda[1,2]
[1]*Department of Physics, University of Tokyo, 7-3-1 Hongo, Bunkyo-ku, Tokyo 113-0033, Japan*
[2]*RIKEN Center for Emergent Matter Science (CEMS), Wako, Saitama 351-0198, Japan*

(Received 17 October 2017; revised manuscript received 29 March 2018; published 19 December 2018)

We unveil the stable $(d+1)$-dimensional topological structures underlying the quench dynamics for all of the Altland-Zirnbauer classes in $d=1$ dimension, and we propose to detect such dynamical topology from the time evolution of entanglement spectra. Focusing on systems in classes BDI and D, we find crossings in single-particle entanglement spectra for quantum quenches between different symmetry-protected topological phases. The entanglement-spectrum crossings are shown to be stable against symmetry-preserving disorder and faithfully reflect both $\mathbb{Z}$ (class BDI) and $\mathbb{Z}_2$ (class D) topological characterizations. As a by-product, we unravel the topological origin of the global degeneracies temporarily emerging in the many-body entanglement spectrum in the quench dynamics of the transverse-field Ising model. These findings can experimentally be tested in ultracold atoms and trapped ions with the help of cutting-edge tomography for quantum many-body states. Our work paves the way towards a systematic understanding of the role of topology in quench dynamics.

DOI: 10.1103/PhysRevLett.121.250601

Introduction.—Topological quantum systems have attracted growing theoretical and experimental interest [1,2], due partly to their fundamental importance in phase transitions beyond the conventional symmetry-breaking paradigm [3] and applications to quantum computation [4–7]. For gapped free-fermion systems at equilibrium, a systematic classification has been established for the Altland-Zirnbauer (AZ) classes [8–12] and with additional crystalline symmetries [13–17]. Topological phases are characterized by topological invariants, some of which have been measured in ultracold atomic gases [18–20]. Entanglement measures [21–23], which are related to the full *entanglement spectrum* (ES) [24–26], provide yet another powerful tool to detect topological order.

Recently, studies on topological systems have been extended to a nonequilibrium regime [27]. Floquet systems [28] have been demonstrated to exhibit intrinsically nonequilibrium topological phases with no static counterparts [29–36]. This Letter focuses on quantum quenches in topological systems [37–46]. Starting from the ground state $|\Psi\rangle$ of an initial Hamiltonian $\hat{H}$, we suddenly change the Hamiltonian to $\hat{H}'$. The wave function subsequently undergoes a nontrivial unitary evolution $|\Psi(t)\rangle = e^{-i\hat{H}'t}|\Psi\rangle$. Previous studies have unveiled topological dynamical phase transitions [39–41], a nonequilibrium Hall response, which is not associated with the Chern number [42–44], and momentum-time Hopf links upon quenches during which the Chern number varies [45,46]. Floquet quenches have also been investigated [47–49].

However, *systematically* identifying and detecting the topology of quench dynamics, i.e., the $(d+1)$-dimensional *spatiotemporal* topology of the wave function, remains an open problem. It is even unclear whether there is a *stable* nontrivial $(d+1)$-dimensional dynamical topology that survives additional bands and disorder. Note that, the Hopf link identified in Ref. [45] is well-defined only for a clean system with two bands [50]. In this Letter, we demonstrate the existence of stable topological structures in quench dynamics, and we propose the time evolution of ES as their universal indicator. We use the K-theory to identify *all* of the AZ classes that accommodate stable nontrivial $(1+1)$-dimensional dynamical topology (see Table I). We generalize the ES approach to quench dynamics, and we perform detailed model studies on topological systems in classes BDI and D, finding robust $\mathbb{Z}$ and $\mathbb{Z}_2$ topological features. Our study has a strong relevance to state-of-the-art

TABLE I. Topological classification of the parent Hamiltonians $\hat{H}(t)$ (1) for quench dynamics. With symmetry constraints (2) alone, the classification is given by the maximal K group, of which only a subset is dynamically realizable (third column).

Altland-Zirnbauer class	Maximal K group	Dynamical realization
A	$\mathbb{Z}$	0
AIII	$\mathbb{Z}\oplus\mathbb{Z}$	$\mathbb{Z}$
AI	0	0
BDI	$\mathbb{Z}$	$\mathbb{Z}$
D	$\mathbb{Z}_2$	$\mathbb{Z}_2$
DIII	$\mathbb{Z}_2\oplus\mathbb{Z}_2$	$\mathbb{Z}_2$
AII	$\mathbb{Z}_2$	0
CII	$\mathbb{Z}$	$\mathbb{Z}$
C	0	0
CI	0	0

 © 2018 American Physical Society

experiments of ultracold atoms [51–55] and trapped ions [56–59], where many-body tomography has become possible [46,60–64].

Parent Hamiltonian and its classification.—For a formal classification, we note that the instantaneous many-body wave function $|\Psi(t)\rangle$ may be regarded as the ground state of

$$\hat{H}(t) \equiv e^{-i\hat{H}'t}\hat{H}e^{i\hat{H}'t}, \tag{1}$$

which we call the *parent Hamiltonian*. Assuming that $\hat{H}$ and $\hat{H}'$ belong to the same d-dimensional AZ class, we obtain

$$\hat{\mathcal{T}}\,\hat{H}(t)\hat{\mathcal{T}}^{-1} = \hat{H}(-t), \qquad \hat{\mathcal{C}}\,\hat{H}(t)\hat{\mathcal{C}}^{-1} = -\hat{H}(t), \\ \hat{\Gamma}\,\hat{H}(t)\hat{\Gamma}^{-1} = -\hat{H}(-t), \tag{2}$$

whenever $\hat{H}$ and $\hat{H}'$ respect the time-reversal symmetry (TRS) $\hat{\mathcal{T}}$, the particle-hole symmetry (PHS) $\hat{\mathcal{C}}$ and/or the chiral symmetry $\hat{\Gamma}$. Regarding t as an extra quasimomentum, we find that $\hat{H}(t)$ respects the TRS in $d+1$ dimensions, but that it respects the PHS and/or the chiral symmetry *only after reversing t to $-t$*. Accordingly, the topological classification for $\hat{H}(t)$ subject to Eq. (2) can differ qualitatively from that for the $(d+1)$-dimensional AZ classes [14]. For $d=1$, the results are shown in the second column in Table I [65]. We emphasize that the *K theory* classification, which has widely been applied to static topological insulators and superconductors [10,12,14,16,17], places no constraints on the number of bands, and the topology is expected to be robust against not-too-strong disorder [69,70]. Here, the disorder can stem not only from the absence of translation invariance in $\hat{H}$ and/or $\hat{H}'$ but also from the *frequency domain* (Fourier transformation of time) due to the band nonflatness in $\hat{H}'$ [71]. These results can straightforwardly be generalized to quench dynamics in higher dimensions and/or with any additional twofold symmetries [14].

At this stage, it is unclear whether a nontrivial element in these maximal K groups can be realized by parent Hamiltonians (1), which have a specific t dependence. After a one-by-one examination [65], we identify all of the dynamically realizable elements in the third column in Table I. It turns out that, for all the nontrivial AZ classes, the *two-dimensional* topological index, i.e., *the strong topological number* [10] of $\hat{H}(t)$ in Eq. (1), is simply the difference between the one-dimensional topological indices of H and H'. This is why the results coincide with the one-dimensional column in the well-known periodic table [8–11]. For example, the strong topological number $\mathbb{Z}$ of $\hat{H}(t)$ in class BDI is given by

$$\Delta w = w' - w, \tag{3}$$

where w (w') is the winding numbers of $\hat{H}$ ($\hat{H}'$). The $\mathbb{Z}_2$ index v of $\hat{H}(t)$ in class D, as first identified in adiabatic PHS-protected pumps [12], is given by

$$v = |\mathcal{N}' - \mathcal{N}|, \tag{4}$$

where $\mathcal{N}$ ($\mathcal{N}'$) is the $\mathbb{Z}_2$ index of $\hat{H}$ ($\hat{H}'$). We will illustrate these two classes with concrete models.

Two remarks are in order. First, the topological numbers in the maximal K groups that are absent in quench dynamics can take nonzero values in adiabatic topological pumps [72–75]. Second, the *weak topological numbers* [10] of a lower-dimensional nature are not shown in Table I. In fact, the conserving Chern number in quench dynamics in two dimensions found in Refs. [38,47] gives such an example. Here, we find another example—the $\mathbb{Z}_2$ index of one-dimensional systems in class D. In other classes, however, the one-dimensional topological index may change or become ill-defined in quench dynamics [76].

Entanglement-spectrum dynamics after quench.—With the topology of quench dynamics formally identified, it is natural to ask how to detect it in a way that is universal, numerically tractable, and experimentally accessible. For static free-fermion systems $\hat{H} = \sum_{j,l,\alpha,\beta} H_{j\alpha,l\beta}\hat{c}^\dagger_{j\alpha}\hat{c}_{l\beta}$, where $\hat{c}^\dagger_{j\alpha}$ creates a particle with internal degrees of freedom α at site j, an ideal candidate is the *single-particle ES*, which gives the *exact* open-boundary spectrum of the flattened Hamiltonian [26]. As for quench dynamics, the *time evolution of ES* thus faithfully simulates the edge spectrum flow under open-boundary conditions in real space. Given the *bulk-edge correspondence* [69], we expect that the dynamical topology can directly be readout from the ES dynamics. Note that, the converse use of this idea can be practically useful for recovering the Hamiltonian topology from quench dynamics, provided that the many-body tomography for $|\Psi(t)\rangle$ [60,63] or the direct measurement of the ES [54,77] is achievable.

We sketch out the definition of the single-particle ES of a Gaussian state $|\Psi\rangle$. Denoting S ($\bar{S}$) as the region of interest (the complement of S), the reduced density operator $\hat{\rho}_S \equiv \mathrm{Tr}_{\bar{S}}[|\Psi\rangle\langle\Psi|]$ can be rewritten as $\hat{\rho}_S = Z_{\mathrm{E}}^{-1}e^{-\hat{H}_{\mathrm{E}}}$, with $\hat{H}_{\mathrm{E}} = \sum_n \epsilon_n \hat{f}^\dagger_n \hat{f}_n$ being the quadratic entanglement Hamiltonian [78], where $\hat{f}_n$ is linear in $\hat{c}_{j\alpha}$. The single-particle ES is given by [79]

$$\xi_n \equiv \frac{1}{e^{\epsilon_n}+1}, \tag{5}$$

so that an entanglement zero mode $\epsilon_n = 0$ corresponds to $\xi_n = \frac{1}{2}$. To investigate the ES dynamics, we calculate ξ_n for $|\Psi(t)\rangle$ at each time in concrete models, in classes BDI and D, and we visualize the $\mathbb{Z}$ and $\mathbb{Z}_2$ indices.

Two-band BDI systems in one dimension.—We start with two-band systems in class BDI. Without the loss of

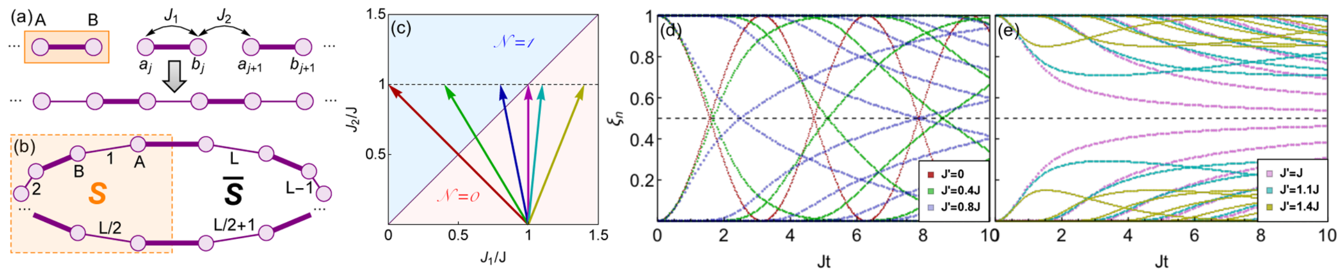

FIG. 1. (a) Quench in the SSH model (6) from a dimerized state. The orange rectangle marks a unit cell. (b) Half-chain entanglement cut (shaded region S) of a periodic chain. (c) Quench protocols. The leftmost three arrows show quenches across the topological phase boundary. (d) Dynamics of the single-particle ES (5) after quenches across the phase boundary, showing crossings at $\xi_n = \frac{1}{2}$. The total number of ξ_n's is L, and most of them are very close to 0 or 1. (e) Single-particle ES dynamics after quenches within the same phase and to the critical point, showing no crossings at $\xi_n = \frac{1}{2}$. The system size is $L = 100$.

generality, we denote the Bloch Hamiltonian as $h(k) = \mathbf{d}(k) \cdot \boldsymbol{\sigma}$, where $\boldsymbol{\sigma} \equiv \sum_{\mu=x,y,z} \sigma^\mu \mathbf{e}_\mu$ is the Pauli-matrix vector, with $\mathbf{e}_\mu$ being the unit vector in the μ direction. The Hamiltonian $\hat{H}$ can be related to $h(k)$ by $\hat{H} = \sum_k \hat{\boldsymbol{c}}_k^\dagger h(k) \hat{\boldsymbol{c}}_k$, where $\hat{\boldsymbol{c}}_k \equiv (\hat{a}_k, \hat{b}_k)^{\mathrm{T}}$, $\hat{a}_k \equiv \frac{1}{\sqrt{L}} \sum_j e^{-ikj} \hat{a}_j$ ($\hat{b}_k \equiv \frac{1}{\sqrt{L}} \sum_j e^{-ikj} \hat{b}_j$), L is the number of unit cells and $\hat{a}_j$ ($\hat{b}_j$) annihilates a fermion in the A (B) sublattice in the jth unit cell [see Fig. 1(a)].

Now we impose TRS $\hat{\mathcal{T}}$ and PHS $\hat{\mathcal{C}}$, which satisfy $\hat{\mathcal{T}}^2 = \hat{\mathcal{C}}^2 = 1$, $\hat{\mathcal{T}} \hat{\mathbf{c}}_k \hat{\mathcal{T}}^{-1} = \hat{\mathbf{c}}_{-k}$ and $\hat{\mathcal{C}} \hat{\boldsymbol{c}}_k \hat{\mathcal{C}}^{-1} = \sigma^z \hat{\boldsymbol{c}}_{-k}$. In terms of the $\mathbf{d}$ vector, the symmetry constraints $[\hat{H}, \hat{\mathcal{T}}] = \{\hat{H}, \hat{\mathcal{C}}\} = 0$ imply $d_x(k) = d_x(-k)$, $d_y(k) = -d_y(-k)$ and $d_z(k) = 0$. Note that, $[\sigma^x, h(\Gamma)] = 0$ at high-symmetry points $\Gamma = 0, \pi$, where the Bloch state is an eigenstate of σ^x with eigenvalue $\nu_\Gamma = \pm 1$. The winding number is determined by $w \equiv \int_{-\pi}^{\pi} (dk/2\pi)(q'(k)/q(k))$ with $q(k) \equiv d_x(k) - i d_y(k)$, and the PHS-protected $\mathbb{Z}_2$ index reads $\mathcal{N} \equiv \frac{1}{2} |\nu_0 - \nu_\pi| = w \bmod 2$.

A prototypical example in class BDI is the Su-Schrieffer-Heeger (SSH) model [80]:

$$\hat{H} = -\sum_j (J_1 \hat{b}_j^\dagger \hat{a}_j + J_2 \hat{a}_{j+1}^\dagger \hat{b}_j + \mathrm{H.c.}), \tag{6}$$

where J_1 and J_2 are the intra- and inter-unit-cell hopping amplitudes, respectively. The Fourier transformation of Eq. (6) gives $\boldsymbol{d}(k) = -(J_1 + J_2 \cos k, J_2 \sin k, 0)$, implying $(\nu_0, \nu_\pi) = [(J_1 + J_2/|J_1 + J_2|), (J_1 - J_2/|J_1 - J_2|))$. In real systems such as polyacetylene [81] and ultracold atoms [18,74,75], we generally have J_1, $J_2 > 0$, and a topological phase transition from $\mathcal{N} = 0$ to $\mathcal{N} = 1$ occurs upon crossing the boundary $J_1 = J_2$ [see Fig. 1(c)].

If we quench the parameters in the SSH model (6) as $(J_1, J_2) = (J, 0) \to (J', J)$, $|\Psi(t)\rangle$ will remain to be in the same trivial phase as the dimerized phase with $\mathcal{N} = 0$. Hence, topological entanglement edge modes in $|\Psi(t)\rangle$ are absent in general. This is confirmed numerically, i.e., the half-chain [see Fig. 1(b)] ES $\xi_n \neq \frac{1}{2}$ for almost all the time in Figs. 1(d) and 1(e). However, in the flat-band case $J' = 0$, we find periodic oscillations of ξ_n's, which cross each other at $t_m = (m - \frac{1}{2}) \frac{\pi}{J}$ with $m \in \mathbb{Z}^+$, where the system instantaneously becomes class BDI with winding number 2. Remarkably, the crossings stay robust as J' increases as long as $J' < J$, with t_1 gradually increasing to infinity. This should be understood as the robustness of the nontrivial $(1+1)$-dimensional topology characterized by $\Delta w = 1$, although the temporal periodicity disappears. When J exceeds J', no crossings occur. This sharp transition in the ES dynamics distinguishes the quenches across different topological phases from those within the same phase.

The ES crossings can alternatively be interpreted as a result of the nontrivial PHS-protected index $v = 1$, which equals the Skyrmion charge (Chern number) of the $\mathbf{d}$-vector textures in one half of the momentum-time space [65]. Indeed, the ES crossings resemble the Dirac-cone dispersion of edge (entanglement) modes in two-dimensional topological insulators [82,83]. The Chern number can be nonzero since d_z is dynamically generated even if it vanishes in both $h(k)$ and $h'(k)$. Such a dynamical Chern number has recently been identified for general two-band systems [84], and it should be experimentally measurable with the help of Bloch-state tomography for ultracold atoms in optical lattices [46,60–62].

Influence of the band number, disorder, and symmetry breaking.—In the presence of additional bands and/or disorder, the picture of momentum-time Skyrmions mentioned above breaks down and only a $\mathbb{Z}_2$ index instead of a PHS-protected Chern number is well-defined. Nevertheless, we will show that the ES dynamics remains a good indicator for the stable dynamical topology and clearly distinguishes the $\mathbb{Z}$ (class BDI) characterization from the $\mathbb{Z}_2$ (class D) one.

According to Table I, the quench dynamics in class BDI systems are characterized by $\mathbb{Z}$. Since the addition operation on a K group is the direct sum up to continuous deformation, we expect the number of ES crossings to be multiplied by M if we quench M copies of the system coupled to each other

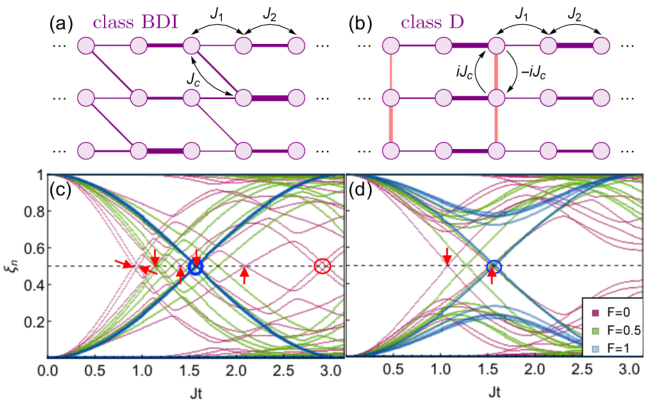

FIG. 2. Three coupled SSH chains in (a) class BDI and (b) class D. Hopping amplitudes J_α ($\alpha = 1, 2, c$) are randomly sampled from a uniform distribution over $[0.6\bar{J}_\alpha, 1.4\bar{J}_\alpha]$. (c) ES dynamics after quench $(\bar{J}_1, \bar{J}_2, \bar{J}_c) = (0, 1.5J, 0) \to (1.5J, 0.5J, 0.5J)$ in (a) with $L = 40$ and the periodic-boundary condition. The result ($F = 0$) is compared with those after partial ($F = 0.5$) and complete ($F = 1$) band flattening $\hat{H}'$. A partially flattened Hamiltonian $\hat{H}'_F$ ($F \in (0, 1)$) is related to the original one $\hat{H}'_0 = \hat{H}'$ and the completely flattened one $\hat{H}'_1$ via $\hat{H}'_F = F\hat{H}'_1 + (1 - F)\hat{H}'_0$. The ES crossings in the blue circle split into those marked by red arrows when F changes from 1 to 0. The remaining two crossings in the red circle occur in the second period in the flat-band limit. (d) Same as (c) but for the system in (b) with a different quench protocol $(\bar{J}_1, \bar{J}_2, \bar{J}_c) = (0, 1.5J, 0) \to (1.5J, 0.5J, J)$.

without breaking the symmetries [see Fig. 2(a)], provided that the disorder in the frequency domain due to band nonflatness is not so strong. We numerically confirm this for $M = 1 \sim 4$ SSH chains with hopping disorder [65]. An example for $M = 3$ is shown in Fig. 2(c), where we see $2M = 6$-fold degenerate ES crossings in the flat-band limit, with the factor of 2 arising from the periodic-boundary condition. Note that, the crossings for nonflat bands are more like middle-gap edge states, a feature well-known in topological crystalline systems [79]. Indeed, $\hat{\mathcal{C}}$ behaves like a crystalline symmetry.

If we break TRS alone, the symmetry class changes from BDI to D and the K-theory classification gives $\mathbb{Z}_2$ (see Table I), over which $1_{\mathbb{Z}_2} + 1_{\mathbb{Z}_2} = 0_{\mathbb{Z}_2}$. As a result, we expect the presence (absence [85]) of ES crossings if we quench odd (even) copies of SSH chains with coupling amplitudes respecting PHS but breaking TRS [see Fig. 2(b)]. In Fig. 2(d), we present the results for $M = 3$ chains. We find that only a single pair of crossings survive in a period in the flat-band limit, and the crossings persist when introducing band nonflatness. We have observed a similar behavior in class DIII [65], which is also characterized by $\mathbb{Z}_2$ (see Table I).

Discussions.—The ES dynamics has been discussed in the transverse-field Ising model [86], which can be mapped to the Kitaev chain [87]. Therein, *global* twofold degeneracies emerge in the many-body ES λ_s's at certain times upon the field quench across the critical value. Since the many-body ES $\{\lambda_s\}$ as eigenvalues of $\hat{\rho}_S$ are related to ξ_n's via [26]

$$\lambda_{s=\{s_n\}} = \prod_n \left[\frac{1}{2} + s_n\left(\xi_n - \frac{1}{2}\right)\right], \qquad s_n = \pm 1, \quad (7)$$

we can attribute these global degeneracies to single-particle ES crossings at $\frac{1}{2}$. Since the Kitaev chain belongs to class D, according to Table I, we expect the global many-body ES degeneracies to be robust against disorder. This is confirmed in an Ising chain subject to an inhomogeneous magnetic field:

$$\hat{H} = \sum_j (J\hat{\sigma}^x_j\hat{\sigma}^x_{j+1} + B_j\hat{\sigma}^z_j), \quad (8)$$

where B_j obeys a uniform distribution over $[\bar{B}_j - W, \bar{B}_j + W]$. As shown in Fig. 3(b), the global many-body ES degeneracies persist in spite of disorder, although they appear at different times. We have further checked the robustness against random coupling [65]. Such a topological dynamical phenomena can be explored in trapped-ion systems with the help of matrix-product-state tomography [63,64].

It was conjectured [86] that the emergence of many-body-ES degeneracies is related to a dynamical quantum phase transition [88] associated with singularities of the dynamical free-energy density $f(t) \equiv -\lim_{L\to\infty}(1/L)\times \ln|\langle\Psi|e^{-i\hat{H}'t}|\Psi\rangle|^2$. As for the SSH model, every time $f(t)$ becomes nonanalytic, we arrive at the center of a momentum-time Skyrmion. However, a precise numerical analysis indicates that these times do not exactly coincide with those of ES crossings [65]. Furthermore, a dynamical phase transition may occur without ES crossings in the Rice-Mele model [89]. Therefore, dynamical phase transitions and ES crossings are not equivalent, although there could be a sufficient condition for both of them [41].

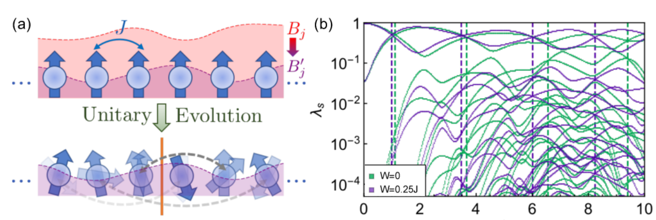

FIG. 3. (a) With an inhomogeneous magnetic field quenched, a nearly disentangled paramagnetic Ising chain (8) becomes entangled under unitary evolution. The orange line denotes the half-chain cut. (b) Dynamics of the many-body ES λ_s (7). Quench protocol: $(J, \bar{B}_j) = (1, 1.5) \to (1, 0.5)$, with $(W = 0.25J)$ or without disorder $(W = 0)$. The length of the open Ising chain is $L = 10$. The dashed lines indicate where global twofold degeneracies emerge.

Similar conclusions are drawn in Ref. [45] for quench dynamics in two dimensions.

The ES dynamics has also been studied in the context of topological Floquet systems [35,90]. A prototypical example of a modulated Ising chain is studied in Ref. [35], which is reminiscent of a quench $\hat{H} = \sum_j B_j \hat{\sigma}_j^z \to \hat{H}' = J\sum_j \hat{\sigma}_j^x \hat{\sigma}_{j+1}^x$ in a single period. However, in Ref. [35], the ES dynamics is for *Floquet eigenstates* and the robustness of crossing is discussed through perturbations with the same Floquet period; here, we focus on physical states undergoing unitary evolution generated by time-independent Hamiltonians, and the temporal periodicity is generally absent.

Summary and outlook.—We have identified the stable topological structures for all the one-dimensional quench dynamics within the same AZ class. We have proposed using the ES dynamics to detect the dynamical topology and performed detailed model studies for classes BDI and D. We have numerically demonstrated the robust $\mathbb{Z}$ and $\mathbb{Z}_2$ features. These phenomena can be explored in state-of-the-art ultracold-atom and trapped-ion experiments [65].

In higher dimensions [91], and/or with additional symmetries, there remains an open problem as to whether a nontrivial $(d+1)$-dimensional topological structure emerges in quench dynamics, and if so, how do the single-particle ES dynamics look. The influence of the interaction is another important issue that might be tackled from the dynamics of the many-body ES. In one dimension, this can be readout from the matrix-product-state representation [92]. Examples are provided in the Supplemental Material [65].

We acknowledge K. Shiozaki, S. Furukawa, M. Sato, S. Higashikawa, Y. Ashida, and M. Nakagawa for valuable discussions. This work was supported by KAKENHI Grant No. JP18H01145 and a Grant-in-Aid for Scientific Research on Innovative Areas “Topological Materials Science” (KAKENHI Grant No. JP15H05855) from the Japan Society for the Promotion of Science. Z. G. was supported by MEXT.

[1] M. Z. Hasan and C. L. Kane, Rev. Mod. Phys. **82**, 3045 (2010).
[2] X.-L. Qi and S.-C. Zhang, Rev. Mod. Phys. **83**, 1057 (2011).
[3] X.-G. Wen, *Quantum Field Theory of Many-Body Systems* (Oxford University Press, New York, 2004).
[4] C. Nayak, S. H. Simon, A. Stern, M. Freedman, and S. Das Sarma, Rev. Mod. Phys. **80**, 1083 (2008).
[5] M. Sato, Y. Takahashi, and S. Fujimoto, Phys. Rev. Lett. **103**, 020401 (2009).
[6] J. D. Sau, R. M. Lutchyn, S. Tewari, and S. Das Sarma, Phys. Rev. Lett. **104**, 040502 (2010).
[7] J. Alicea, Y. Oreg, G. Refael, F. von Oppen, and M. P. A. Fisher, Nat. Phys. **7**, 412 (2011).
[8] A. Altland and M. R. Zirnbauer, Phys. Rev. B **55**, 1142 (1997).
[9] A. P. Schnyder, S. Ryu, A. Furusaki, and A. W. W. Ludwig, Phys. Rev. B **78**, 195125 (2008).
[10] A. Kitaev, AIP Conf. Proc. **1134**, 22 (2009).
[11] S. Ryu, A. P. Schnyder, A. Furusaki, and A. W. W. Ludwig, New J. Phys. **12**, 065010 (2010).
[12] J. C. Y. Teo and C. L. Kane, Phys. Rev. B **82**, 115120 (2010).
[13] C.-K. Chiu, H. Yao, and S. Ryu, Phys. Rev. B **88**, 075142 (2013).
[14] K. Shiozaki and M. Sato, Phys. Rev. B **90**, 165114 (2014).
[15] Y. Ando and L. Fu, Annu. Rev. Condens. Matter Phys. **6**, 361 (2015).
[16] K. Shiozaki, M. Sato, and K. Gomi, Phys. Rev. B **93**, 195413 (2016).
[17] C.-K. Chiu, J. C. Y. Teo, A. P. Schnyder, and S. Ryu, Rev. Mod. Phys. **88**, 035005 (2016).
[18] M. Atala, M. Aidelsburger, J. T. Barreiro, D. Abanin, T. Kitagawa, E. Demler, and I. Bloch, Nat. Phys. **9**, 795 (2013).
[19] M. Aidelsburger, M. Lohse, C. Schweizer, M. Atala, J. T. Barreiro, S. Nascimbène, N. R. Cooper, I. Bloch, and N. Goldman, Nat. Phys. **11**, 162 (2015).
[20] N. R. Cooper, J. Dalibard, and I. B. Spielman, arXiv:1803.00249.
[21] A. Kitaev and J. Preskill, Phys. Rev. Lett. **96**, 110404 (2006).
[22] M. Levin and X.-G. Wen, Phys. Rev. Lett. **96**, 110405 (2006).
[23] S. T. Flammia, A. Hamma, T. L. Hughes, and X.-G. Wen, Phys. Rev. Lett. **103**, 261601 (2009).
[24] H. Li and F. D. M. Haldane, Phys. Rev. Lett. **101**, 010504 (2008).
[25] F. Pollmann, A. M. Turner, E. Berg, and M. Oshikawa, Phys. Rev. B **81**, 064439 (2010).
[26] L. Fidkowski, Phys. Rev. Lett. **104**, 130502 (2010).
[27] J. Eisert, M. Friesdorf, and C. Gogolin, Nat. Phys. **11**, 124 (2015).
[28] R. Moessner and S. L. Sondhi, Nat. Phys. **13**, 424 (2017).
[29] T. Kitagawa, E. Berg, M. Rudner, and E. Demler, Phys. Rev. B **82**, 235114 (2010).
[30] L. Jiang, T. Kitagawa, J. Alicea, A. R. Akhmerov, D. Pekker, G. Refael, J. I. Cirac, E. Demler, M. D. Lukin, and P. Zoller, Phys. Rev. Lett. **106**, 220402 (2011).
[31] M. S. Rudner, N. H. Lindner, E. Berg, and M. Levin, Phys. Rev. X **3**, 031005 (2013).
[32] F. Nathan and M. S. Rudner, New J. Phys. **17**, 125014 (2015).
[33] P. Titum, E. Berg, M. S. Rudner, G. Refael, and N. H. Lindner, Phys. Rev. X **6**, 021013 (2016).
[34] V. Khemani, A. Lazarides, R. Moessner, and S. L. Sondhi, Phys. Rev. Lett. **116**, 250401 (2016).
[35] A. C. Potter, T. Morimoto, and A. Vishwanath, Phys. Rev. X **6**, 041001 (2016).
[36] H. C. Po, L. Fidkowski, T. Morimoto, A. C. Potter, and A. Vishwanath, Phys. Rev. X **6**, 041070 (2016).
[37] M. S. Foster, M. Dzero, V. Gurarie, and E. A. Yuzbashyan, Phys. Rev. B **88**, 104511 (2013).

[38] M. D. Caio, N. R. Cooper, and M. J. Bhaseen, Phys. Rev. Lett. **115**, 236403 (2015).
[39] S. Vajna and B. Dóra, Phys. Rev. B **91**, 155127 (2015).
[40] J. C. Budich and M. Heyl, Phys. Rev. B **93**, 085416 (2016).
[41] Z. Huang and A. V. Balatsky, Phys. Rev. Lett. **117**, 086802 (2016).
[42] Y. Hu, P. Zoller, and J. C. Budich, Phys. Rev. Lett. **117**, 126803 (2016).
[43] J. H. Wilson, J. C. W. Song, and G. Refael, Phys. Rev. Lett. **117**, 235302 (2016).
[44] M. D. Caio, N. R. Cooper, and M. J. Bhaseen, Phys. Rev. B **94**, 155104 (2016).
[45] C. Wang, P. Zhang, X. Chen, J. Yu, and H. Zhai, Phys. Rev. Lett. **118**, 185701 (2017).
[46] M. Tarnowski, F. N. Ünal, N. Fläschner, B. S. Rem, A. Eckardt, K. Sengstock, and C. Weitenberg, arXiv:1709.01046.
[47] L. D'Alessio and M. Rigol, Nat. Commun. **6**, 8336 (2015).
[48] D. J. Yates, Y. Lemonik, and A. Mitra, Phys. Rev. B **94**, 205422 (2016).
[49] D. J. Yates and A. Mitra, Phys. Rev. B **96**, 115108 (2017).
[50] J. E. Moore, Y. Ran, and X.-G. Wen, Phys. Rev. Lett. **101**, 186805 (2008).
[51] T. Langen, R. Geiger, and J. Schmiedmayer, Annu. Rev. Condens. Matter Phys. **6**, 201 (2015).
[52] A. J. Daley, H. Pichler, J. Schachenmayer, and P. Zoller, Phys. Rev. Lett. **109**, 020505 (2012).
[53] R. Islam, R. Ma, P. M. Preiss, M. E. Tai, A. Lukin, M. Rispoli, and M. Greiner, Nature (London) **528**, 77 (2015).
[54] H. Pichler, G. Zhu, A. Seif, P. Zoller, and M. Hafezi, Phys. Rev. X **6**, 041033 (2016).
[55] H. Bernien, S. Schwartz, A. Keesling, H. Levine, A. Omran, H. Pichler, S. Choi, A. S. Zibrov, M. Endres, M. Greiner, V. Vuletić, and M. D. Lukin, Nature (London) **551**, 579 (2017).
[56] S. Korenblit, D. Kafri, W. C. Campbell, R. Islam, E. E. Edwards, Z.-X. Gong, G.-D. Lin, L.-M. Duan, J. Kim, K. Kim, and C. Monroe, New J. Phys. **14**, 095024 (2012).
[57] J. Smith, A. Lee, P. Richerme, B. Neyenhuis, P. W. Hess, P. Hauke, M. Heyl, D. A. Huse, and C. Monroe, Nat. Phys. **12**, 907 (2016).
[58] P. Jurcevic, H. Shen, P. Hauke, C. Maier, T. Brydges, C. Hempel, B. P. Lanyon, M. Heyl, R. Blatt, and C. F. Roos, Phys. Rev. Lett. **119**, 080501 (2017).
[59] J. Zhang, G. Pagano, P. W. Hess, A. Kyprianidis, P. Becker, H. Kaplan, A. V. Gorshkov, Z.-X. Gong, and C. Monroe, Nature (London) **551**, 601 (2017).
[60] P. Hauke, M. Lewenstein, and A. Eckardt, Phys. Rev. Lett. **113**, 045303 (2014).
[61] N. Fläschner, B. S. Rem, M. Tarnowski, D. Vogel, D.-S. Lühmann, K. Sengstock, and C. Weitenberg, Science **352**, 1091 (2016).
[62] N. Fläschner, D. Vogel, M. Tarnowski, B. S. Rem, D.-S. Lühmann, M. Heyl, J. C. Budich, L. Mathey, K. Sengstock, and C. Weitenberg, Nat. Phys. **14**, 265 (2018).
[63] M. Cramer, M. B. Plenio, S. T. Flammia, R. Somma, D. Gross, S. D. Bartlett, O. Landon-Cardinal, D. Poulin, and Y.-K. Liu, Nat. Commun. **1**, 149 (2010).
[64] B. P. Lanyon, C. Maier, M. Holzäpfel, T. Baumgratz, C. Hempel, P. Jurcevic, I. Dhand, A. S. Buyskikh, A. J. Daley, M. Cramer, M. B. Plenio, R. Blatt, and C. F. Roos, Nat. Phys. **13**, 1158 (2017).
[65] See Supplemental Material at http://link.aps.org/supplemental/10.1103/PhysRevLett.121.250601, which includes Refs. [66–68], for the details.
[66] J. E. Moore and L. Balents, Phys. Rev. B **75**, 121306(R) (2007).
[67] L. Fu and C. L. Kane, Phys. Rev. B **76**, 045302 (2007).
[68] A. T. Sornborger and E. D. Stewart, Phys. Rev. A **60**, 1956 (1999).
[69] E. Prodan and H. Schulz-Baldes, *Bulk and Boundary Invariants for Complex Topological Insulators: From K-Theory to Physics* (Springer, Berlin, 2016).
[70] G. C. Thiang, Ann. Inst. Henri Poincaré **17**, 757 (2016).
[71] The initial ground state stays unchanged if we flatten $\hat{H}$.
[72] D. J. Thouless, Phys. Rev. B **27**, 6083 (1983).
[73] L. Fu and C. L. Kane, Phys. Rev. B **74**, 195312 (2006).
[74] M. Lohse, C. Schweizer, O. Zilberberg, M. Aidelsburger, and I. Bloch, Nat. Phys. **12**, 350 (2016).
[75] S. Nakajima, T. Tomita, S. Taie, T. Ichinose, H. Ozawa, L. Wang, M. Troyer, and Y. Takahashi, Nat. Phys. **12**, 296 (2016).
[76] M. McGinley and N. R. Cooper, Phys. Rev. Lett. **121**, 090401 (2018).
[77] M. Dalmonte, B. Vermersch, and P. Zoller, Nat. Phys. **14**, 827 (2018).
[78] I. Peschel, J. Phys. A **36**, L205 (2003).
[79] T. L. Hughes, E. Prodan, and B. A. Bernevig, Phys. Rev. B **83**, 245132 (2011).
[80] W. P. Su, J. R. Schrieffer, and A. J. Heeger, Phys. Rev. Lett. **42**, 1698 (1979).
[81] H. Shirakawa, E. J. Louis, A. G. MacDiarmid, C. K. Chiang, and A. J. Heeger, J. Chem. Soc. Chem. Commun. 578 (1977).
[82] C. L. Kane and E. J. Mele, Phys. Rev. Lett. **95**, 226801 (2005).
[83] A. M. Turner, Y. Zhang, and A. Vishwanath, Phys. Rev. B **82**, 241102(R) (2010).
[84] C. Yang, L. Li, and S. Chen, Phys. Rev. B **97**, 060304(R) (2018).
[85] We do not rule out the possibility of finding accidental ES crossings without topological origin. Note that edge states may also exist in topologically trivial systems.
[86] G. Torlai, L. Tagliacozzo, and G. D. Chiara, J. Stat. Mech. (2014) P06001.
[87] A. Y. Kitaev, Phys. Usp. **44**, 131 (2001).
[88] M. Heyl, A. Polkovnikov, and S. Kehrein, Phys. Rev. Lett. **110**, 135704 (2013).
[89] M. J. Rice and E. J. Mele, Phys. Rev. Lett. **49**, 1455 (1982).
[90] I.-D. Potirniche, A. C. Potter, M. Schleier-Smith, A. Vishwanath, and N. Y. Yao, Phys. Rev. Lett. **119**, 123601 (2017).
[91] P.-Y. Chang, Phys. Rev. B **97**, 224304 (2018).
[92] G. Vidal, Phys. Rev. Lett. **98**, 070201 (2007).